PNAS
www.pnas.org

Supplementary Information for

The Habenular G-Protein-Coupled Receptor 151 regulates synaptic plasticity and nicotine intake

Beatriz Antolin-Fontes[1], Kun Li[1], Jessica L. Ables[1,2,3], Michael H. Riad[1], Andreas Görlich[1] Maya Williams[2], Cuidong Wang[1], Sylvia M. Lipford[1], Maria Dao[2], Jianxi Liu[4], Henrik Molina[5], Nathaniel Heintz[1], Paul J. Kenny[2,4] and Ines Ibañez-Tallon[1]*

*Corresponding Author: iibanez@rockefeller.edu

This PDF file includes:

Supplementary text
Figures S1 to S11
Tables S1 to S3
Legends for Datasets S1 to S2
SI References

Other supplementary materials for this manuscript include the following:

Datasets S1 to S2

www.pnas.org/cgi/doi/10.1073/pnas.1916132117

SUPPLEMENTARY INFORMATION TEXT

SUPPLEMENTARY EXPERIMENTAL PROCEDURES

Animals

Transgenic *Chat-EGFP-L10a* (*Chat-DW167*) have been previously described [1-4]. Tabac mice expressing the *Chrnβ4-α3-eGFP-α5* gene cluster have been characterized in [2]. *Gpr151* knockout mice (Gpr151tm1Dgen) were obtained from Deltagen (RRID:MGI_3606630). They were backcrossed to C57BL/6 for eight generations. *Chat*-ChR2-YFP BAC transgenic mice were obtained from The Jackson Laboratory (Strain name: B6.Cg-Tg(Chat-COP4*H134R/EYFP)6Gfng/J, RRID:MGI_5491602). All lines were maintained on a heterozygous background.

Drugs

(-) Nicotine hydrogen tartrate salt was purchased from Sigma-Aldrich (St. Louis, MO, USA). Nicotine concentrations refer to the free base. For nicotine self-administration experiments, (-) nicotine hydrogen tartrate salt was dissolved in 0.9% sterile saline for 0.3 mg/ml stock solution. For systemic injections, nicotine was dissolved in sterile water and injected at 10 ml/kg volume. The pH of all solutions was adjusted to approximately 7.4. Isobutylmethylxanthine (IMBX) and forskolin were obtained from Tocris Bioscience and Sigma-Aldrich.

Immunohistochemistry of mouse brain samples and quantification analysis

The primary antibodies used were: rabbit polyclonal anti-GPR151 (1:1000, Sigma, RRID:AB_10743863), goat polyclonal anti-GPR151 (1:500, Santa Cruz, RRID:AB_2113821), goat polyclonal anti-CHAT (1:1000, Millipore, RRID:AB_2079751), chicken polyclonal anti-ß-galactosidase (β-Gal) (1:200, Abcam, RRID:AB_307210), chicken polyclonal anti-GFP (1:1000, Aves, RRID:AB_10000240). The sections were incubated with primary antibodies overnight at 4°C or room temperature. After incubation with secondary antibodies (Jackson ImmunoResearch, PA, USA), sections were washed, mounted on slides and coverslipped in immu-mount (Thermo Scientific, MA, USA). Heat-mediated antigen retrieval, 15 minutes at 95°C in citric acid (pH 6.0), was performed prior to incubation with the choline acetyltransferase (CHAT) antibody. Fluorescent signals were detected using a confocal laser scanning microscope (Zeiss LSM700, Germany).

Image J was used for quantification analysis. The number GPR151 (β-Gal positive) and CHAT cells per section was quantified in 39 habenula of 3 different *Gpr151*-KO mice.
Colocalization analysis was done as described in [5] with the Coloc 2 plugin in the Fiji image processing package. Background was eliminated by median subtraction [6]. Manders' colocalization coefficients (M1 and M2), which are proportional to the number of colocalizing pixels in each channel relative to the total number of pixels, were calculated [7]. M1 or M2 > 0.55 indicates colocalization [8]. In this study, only M1 is presented and refers to the proportion of pixels with GPR151 immunoreactivity that colocalize with the second marker. Costes' test for statistical significance was used to determine that the colocalization coefficients obtained were not due to random effects [9]. This test creates random images by shuffling blocks of pixels of one channel, measuring the correlation of this channel with the other (unscrambled) channel of the same image. The test was performed 100 times per image and the resulted P value indicates the proportion of random images that have better correlation than the real image. A P-value of 1.00 means that none of the randomized images had better correlation.

Co-immunoprecipitation and western blot

The IPN was dissected from 15-20 WT and *Gpr151*-KO mice and homogenized in 500 ul lysis buffer (50 mM Tris-HCl pH 8.0, 100 mM NaCl, 2mM EDTA, 1% Triton-X100, 5% Glycerol and protease and phosphatase inhibitors tablets (Roche) using a tissue grinder. The homogenates were placed on a rotator for 30 min at 4 °C centrifuged for 15 min at 14000 rpm. The supernatant, which contains the cytosolic proteins, was collected and the pellet, which contains the membrane protein, was resuspended in 50-100 ul lysis buffer containing 2% Triton X-100 for 2 hr at 4°C. Samples were centrifuged for 15 min at 14000 rpm and the supernatant was combined with the cytosolic sample.
For co-immunoprecipitation for mass spectrometry analysis, M-270 Epoxy Dynabeads (Invitrogen, MA, USA) were used. Coupling of the antibody to the beads was done as suggested by the manufacturer. A combination of three different GPR151 antibodies (30 µg of rabbit polyclonal anti-GPR151 (Sigma, RRID:AB_10743863), 10 µg of goat polyclonal anti-GPR151 (Santa Cruz, RRID:AB_2113821) and 20 µl of mouse polyclonal anti-GPR151 (Sigma, RRID:AB_10608138) were coupled to 15 mg of beads per sample during 24 hr at 37°C in 1.5 ml volume. After conjugation, beads were washed, added to the sample and incubated for 16 hr on a rotator at 4°C. The beads were subsequently washed six times with lysis buffer (twice with buffer containing Triton-X100 and three

additional times with lysis buffer without Triton-X100). The suspension was then transferred to a clean tube and two serial elutions of the protein complex were performed with 40 ul 8M Urea (freshly prepared) for 30 and 10 min at room temperature on a rotator. The supernatant (80 µl total) was transferred to a new tube and 500 ul of cold acetone was added to precipitate proteins and remove detergent. The sample was kept overnight at -20 °C and centrifuged the following morning at 14000 rpm for 5 min. The acetone was discarded and the pellet was dissolved in 8M urea for mass spectrometry analysis.

For co-immunoprecipitation for western blot analysis, 50 µl of DynaBeads Protein G (Invitrogen) were used per sample according to the manufacturer's recommendations. 5 µg of rabbit polyclonal anti-GPR151 (Sigma, RRID:AB_10743863) and 1 µg of goat polyclonal anti-GPR151 (Santa Cruz, RRID:AB_2113821) were incubated with the beads for 1 hr at room temperature. After washing the beads and antibody complex, the sample was added to the tube and incubated with the beads for 16 hr on a rotator at 4°C. The complex was eluted with 20 µl elution buffer plus 10 µl of NuPAGE LDS sample buffer/reducing agent mix and incubated 10 min at 70 °C. The supernatant was removed and directly loaded onto a NuPAGE Bis–Tris 4–12 % pre-cast gel (100 V, 2 hr). Proteins were transferred onto a PVDF membrane for 90 min at 100 V in the NuPAGE transfer buffer supplemented with 20 % methanol. The membranes were then blocked for 2 h in 5 % BSA in TBS-T and incubated with mouse polyclonal anti-GPR151 (1:1000, Sigma, RRID:AB_10608138), mouse monoclonal anti-Gαo 1/2 (1:1000, Synaptic Systems, #271 111) and rabbit polyclonal anti-Gαs (1:1000, Abcam, RRID:AB_1860300) overnight at 4°C. LI-COR secondary antibodies were used (1:15000) for 1 hr and the membranes were scanned and quantified using the LI-COR Odyssey imaging system (LI-COR Biosciences, NE, USA). Comassie stainings were performed using Coomassie® R-250 (ThermoFisher Scientific) following the manufacturer's instructions.

Proteomics Methods and data Analysis

Ten samples (five biological replicates of each WT and *Gpr*151-KO immunoprecipitation experiments) were denatured in 8M urea, reduced with 10 mM DTT, and alkylated with 50 mM iodoacetamide. This was followed by proteolytic digestion with endoproteinase LysC (Wako Chemicals, VA, USA) overnight, and with trypsin (Promega, WI, USA) for 6h at room temperature. The digestion was quenched with 5% formic acid (final concentration) and resulting peptide mixtures were desalted using in-house made C18 Empore (3M) StAGE tips. Samples were dried and resolubilized in 2% acetonitrile and 2% formic acid.

One fifth of each desalted [10] sample was injected for analysis by reversed phase nano-LC-MS/MS (Ultimate 3000 coupled to a QExactive Plus, Thermo Scientific, MA, USA). After loading on a C18 PepMap trap column (5 µm particles, 100µm x 2 cm, Thermo Scientific, MA, USA) at a flow rate of 3 µl/min, peptides were separated using a 12 cm x 75µm C18 column (3 µm particles, Nikkyo Technos Co., Ltd. Japan) at a flow rate of 200 nL/min, with a gradient increasing from 5% Buffer B (0.1% formic acid in acetonitrile) / 95% Buffer A (0.1% formic acid) to 40% Buffer B / 60% Buffer A, over 140 minutes. All LC-MS/MS experiments were performed in data dependent mode with lock mass of m/z 445.12003. Precursor mass spectra were recorded in a 300-1400 m/z range at 70,000 resolution, and fragment ions at 17,500 resolution (lowest mass: m/z 100) in profile mode. Up to twenty precursors per cycle were selected for fragmentation and dynamic exclusion was set to 60 seconds. Normalized collision energy was set to 27.

Data were quantified and searched against Uniprot mouse database (February 2019) using MaxQuant (version 1.6.0.13) [11]. Oxidation of methionine and protein N-terminal acetylation were allowed as variable modifications, cysteine carbamidomethyl was set as a fixed modification and two missed cleavages were allowed. The “match between runs” option was enabled, and false discovery rates for proteins and peptide spectrum matches were set to 1% and 2%, respectively. Protein abundances were expressed as intensity Based Absolute Quantitation (iBAQ) [12]. In short: LOG2 transformed iBAQ signals were normalized by subtracting median. Identified proteins were further filtered by requiring that at least 3 signals were present for each protein in at least one condition. Missing signals were imputed and the two conditions were compared using a P-value only t-test. Threshold of P>0.05 and a difference of 2 linear folds were set as filters to identify proteins of interest.

Immunohistochemistry and protein extraction of human brain samples

Fixed samples of about 2 cm wide x 5 cm long x 1 cm deep containing the habenula, the fasciculus retroflexus and the interpeduncular nucleus, were cryoprotected for 2 days in sucrose in 15% sucrose and for 2 following days in 30% sucrose. 50 µM sections were sectioned on a SM2000R sliding microtome (Leica, IL, USA). Sections were washed for one hour in 1xPBS containing 0.2%TX100 and then blocked for 2 hours in 1xPBS containing 0.5%TX100 and 4%NDS. Subsequently, sections were incubated overnight at 4 °C with the rabbit polyclonal anti-GPR151 (Sigma, 1:1000, RRID:AB_10743863) diluted in blocking buffer. The following morning, sections were washed with 1xPBS containing 0.2%TX100 and incubated for 2 h at room temperature with secondary antibodies (1:500;

Jackson ImmunoResearch, PA, USA). Sections were mounted on slides and examined and photographed with a LSM700 (Zeiss, Germany) confocal microscope.
For human western blot analysis, the IPN (60-450 mg) was dissected from frozen sections of the midbrain and homogenized using a motor-driven Teflon-glass homogenizer in 500 µl - 1 ml lysis buffer. Cytosolic and membrane protein fractions were used for immunoprecipitation and western blot analysis as described with mouse tissue.

Stereotaxic viral injections

Mice, 8-9 weeks old, were anesthesized with ketamine/xylazine (130 mg/kg and 10 mg/kg, respectively), and placed in a Benchmark stereotaxic frame with a Cunningham mouse adaptor (Leica). The eyes were covered with Regephitel® ointment to prevent desiccation. Four holes were drilled on the skull with a micromotor drill with a 0.35 mm diameter bit. The coordinates used to target the medial habenula were the following: anterior-posterior (from Bregma): -1.4 and -1.75; lateral +/-0.33; dorso-ventral (from the skull) -2.72 and -2.70. Glass PCR micropipets (Drummond) that had been pulled with a microelectrode puller (Narashige) to create a narrow, fine tip of ~10-12 mm length were used for the injections. The cannula was filled from the backside with virus, followed by mineral oil. A metal plunger was inserted into the upper part of the cannula and placed in the stereotaxic apparatus. 0.5-1 µl of virus was injected into the mouse medial habenula using a MO-10 oil hydraulic micromanipulator (Narashige) with a flow rate of ~0.1 µl/min. The cannula was left in place for 5 min, allowing the virus solution to disperse in the tissue, before it was slowly retracted. The incision was closed with the tissue adhesive Vetbond (3M). After surgery, mice were warmed up by the infrared lamp and left for recovery for 2h. Mice were kept under S2 conditions for a week. The following virus were used: AAV2/1-U6-Gpr151-shRNA and AAV2/1-GFP-U6-scramble-shRNA from Vector Biolabs, AAV2/1-CAG-M-Gpr151-WPRE from Vector Biolabs for rescue experiments, AAV2/1-L10a-EGFP control virus from Janelia farms. Viral titers were 10^{13} inclusion forming units (IFU)/mL.

Electron microscopy

Fixation, high pressure freezing and freeze substitution was performed as in [5]. For pre-embedding nanogold immunolabeling, IPN coronal sections from WT and *Gpr151*-KO mice were incubated in blocking solution (3% BSA, 0.1% saponin) for 2 hours at room temperature. The sections were then single labeled at 4°C for 36 hr with rabbit polyclonal anti-GPR151; 1/3000 (Sigma, RRID:AB_10743863) diluted in blocking solution and

incubated in secondary antibody diluted 1:100 for 1hr at room temperature (Nanoprobes-Nanogold, anti-Rabbit: 2003). The sections were fixed in 2.5% glutaraldehyde overnight at 4°C and subsequently underwent silver enhancement (HQ Silver Enhancement 2012, Nanoprobes, NY, USA), and Gold Toning using a 0.1% solution of gold chloride (HT1004, Sigma-Aldrich, MO, USA). The rostral IPN was excised and postfixed with 1% osmium tetroxide in the buffer for 1 hour on ice. Sections underwent *en bloc* staining with 1% uranyl acetate for 30 min, dehydration in a graded series of ethanol, 10 minutes in acetone, infiltration with Eponate 12™ Embedding Kit (Ted Pella, CA, USA), embedding with the resin and polymerization for 48h at 60°C. 70nm ultrathin sections were analyzed on a JEOL JEM-100CX (JEOL, Tokyo, Japan) at 80kV using with the digital imaging system (XR41-C, Advanced Microscopy Technology Corp, Woburn, MA, USA).

Post-embedding immunolabeling was carried out on 90 nm ultrathin sections mounted on carbon film 200 mesh nickel grids (Electron Microscopy Sciences, PA, USA). Sections were incubated in blocking solution containing 3% BSA, 0.1% in 1xPBS for 1h, incubated with single or double primary antibodies: rabbit polyclonal anti-GPR151; 1/800 (Sigma, RRID:AB_10743863) and/or guinea pig polyclonal anti-VGLUT1; 1/400 (Synaptic Systems, RRID:AB_887878) diluted in blocking solution overnight at 4°C, rinsed in blocking solution for 30 min, incubated with appropriate secondary antibodies (e.g., anti-rabbit IgG conjugated to 12 nm gold particles and anti-guinea pig IgG conjugated to 6 nm gold particles (Jackson ImmunoResearch, PA, USA) diluted 1/20 in PBS containing 0.5% BSA and 0.1% saponin for 1h at room temperature. Finally, sections were washed twice in PBS and twice in ultrapure water, stained with1% osmium tetroxide and lead citrate and examined in a JEOL JEM-100CX microscope. The control experiment was done by following the same procedure except for omitting the primary antibody and incubating with blocking solution instead.

Quantitative analyses were performed on preembedding nanogold labeled synaptic terminals (at 10000x magnification) from three WT mice and *Gpr151*-KO mice. 45 terminals with distinguishable active zone and synaptic vesicles of 3 WT and 3 *Gpr151*-KO mice were analyzed to quantify the area of the terminal, length of the active zone, and size, density and distribution of synaptic vesicles. On a separate analysis, 50 terminals of 3 WT mice with a distinguishable active zone and 46 terminals filled with vesicles but without the active zone in the picture were quantified (a total of 999 GPR151 nanogold particles in terminals with AZ and 864 particles in terminals without AZ). All measurements were done with ImageJ.

TRAP and RNA-SEQ

RNA-seq reads were aligned to the UCSC mm10 reference genome using STAR [13], version 2.3.0e_r291, with default settings. Quantification of aligned reads was done using htseq-count module, part of the 'HTSeq' framework [14], version 0.6.0, using default settings, with 'union' mode to handle reads overlapping more than one feature. Differentially expressed genes were identified by performing a negative binomial test using DESeq2 [15] (R-package version 1.4.5) with default settings. Significant P-values were corrected to control the false discovery rate of multiple testing according to the Benjamini-Hochberg [16] procedure at 0.05 threshold. Gene lists were then further filtered for basemean > 100 counts to exclude genes with low expression.

Behavioral analysis

Open field. Locomotor activity was measured in eight identical open field boxes (50x50x22.5 cm) equipped with two rows of infrared photocells placed 20 and 50 mm above the floor (Accuscan & Omnitech Electronics, OH, USA). Mice were placed in the center of the field and activity was recorded by the Fusion Software. To habituate the animals to the test environment and to obtain a stable baseline, locomotor activity was measured immediately after a saline injection for 60 min 2 days before the testing day.
To evaluate the hypolocomotor effects of nicotine (0.65 mg/kg, i.p), mice were placed on open field boxes for 20 min immediately after injection. Tolerance to the locomotor effect of nicotine was measured every other day for 20 min immediately after nicotine injection for 11 days.

Elevated Plus maze. Elevated Plus Maze was used to assess anxiety-like behavior. The apparatus consisted of a central platform (5 × 5 cm), two opposed open arms (25 × 5 cm) and two opposed closed arms with 15-cm-high black walls. The edges of the open arms were raised 0.25 cm to decrease the chance of a mouse falling. Mice were placed on the central platform and the time and activity were recorded for 10 min via a camera positioned above the apparatus. Time spent in each arm and the distance traveled was recorded automatically using EthoVision XT Tracking Software (Noldus, VA, USA).

Prepulse Inhibibition. Startle reflexes were measured in four identical startle response SR-LAB apparatus (San Diego Instruments, CA, USA). Each system contained a Plexiglas

cylinder, 5.5 cm in diameter and 13 cm long, mounted on a platform located in a ventilated, sound-attenuated chamber. Startle responses were transduced by piezoelectric accelerometers mounted under each platform. Output signals were digitized and the average startle response and maximum amplitude of the startle response were recorded as startle units. The startle session began with a 5 min acclimation period in the presence of a 65-dB background white noise, followed by presentation of five 120 dB pulse trials to ensure a stable baseline and reduce variability. Afterwards mice were presented with four startle stimulus of different intensities (80, 90, 100, 110, 120 dB). A total of 20 trials in a pseudo-randomized manner with an average inter-trial-interval of 15 sec (range: 6-21 sec) were presented. Amplitude of startle was measured within a 100 msec window following the stimuli. Prepulse Inhibition was examined using prepulses of 3, 6 or 12 dB (20ms) above background. Testing consisted of twelve 120 dB pulses (40 ms duration) alone and ten pulses preceded (100 ms) by each prepulse (20 ms duration). One last block of five 120 db pulses was presented to ensure again a stable baseline. Percent PPI was calculated using the following formula: 100x(startle alone – startle with prepulse/startle alone). PPI was reported as percent inhibition of the average startle response.

Sucrose preference. It was measured for 24hr. Mice were single-housed and given a free choice between two bottles, one with 2% sucrose and another one with tap water. The solutions were presented in 50 ml falcon tubes containing stoppers fitted with ball–point sipper tubes to prevent leakage. To prevent possible effects of side preference, the position of the bottles was switched after 24 hr and the test was repeated. The preference for sucrose was calculated as a percentage of consumed sucrose solution of the total amount of liquid drunk.

Operant conditioning

Mice were mildly food restricted to 85-90% of free-feeding body weight and trained to respond on one of two levers (active and inactive) in an operant conditioning chamber (10 x 10 x 10 cm chamber in sound attenuating box, Med-Associates Inc., St. Albans, VT, USA) for food pellets (20 mg pellets; TestDiet, Richmond, IN). Mice responded during 1 h daily training sessions (7 sessions per week) until they achieved stable responding under a fixed-ratio 5, time out 20 sec (FR5TO20) schedule of reinforcement. Stable responding was defined as 3 consecutive sessions when mice achieved >25 food pellets/session. To test the effects of nicotine on food responding, mice were injected with saline or nicotine

(1mg/kg, s.c.) 10 min prior to their regular daily session and effects on food responding were measured for 5 min. Nicotine and saline injections were delivered according to an unbiased counterbalanced design.

Jugular catheter surgery

Mice were anesthetized using isoflurane (1-3%)/oxygen vapor mixture and implanted with intravenous catheters. Catheters consisted of 6 cm (mice) length of silastic tubing fitted to a guide cannula (Plastics One, Wallingford, CT), curved to a right angle. Catheter/cannula assemble was encased in dental acrylic with 5 cm of catheter tubing extended from the cannula base. The catheter tubing was surgically impacted via an incision on the animal's back, with the catheter passed subcutaneous to the neck. The catheter was then implanted approximately 1 cm into right jugular vein and secured in place using surgical silk suture. Catheters were flushed daily with physiological sterile saline solution (0.9% w/v) containing heparin (60 USP units/ml). Catheter integrity was tested with the acute reacting barbiturate anesthetic, Brevital (methohexital sodium, Eli Lilly, Indianapolis, IN).

Intravenous nicotine self-administration procedure

When mice demonstrated stable responding in the operant chamber (>25 food pellets per session), they underwent jugular catheter implantation. The animals were permitted at least 48 h to recover from surgery and then permitted to respond for food rewards again under the same FR5TO20 sec schedule. Once stable responding was re-established subjects were permitted to respond for intravenous nicotine infusions during 1 h daily sessions, 7 days per week (0.03 mg/kg/infusion). Nicotine was delivered via the implanted intravenous catheter by a Razel syringe pump (MedAssociates Inc., St Albans VT USA). Completion of the response criteria on the active lever resulted in the delivery of an intravenous nicotine infusion (0.03 ml infusion volume). Responses on the inactive lever were recorded but had no scheduled consequences. Once stable responding at the 0.03 mg/kg/infusion dose was achieved (~5-7 days), animals were then permitted to respond for 0.1 mg/kg/infusion dose of nicotine (training dose) for at least 7 days prior to the start of dose-response assessment. For dose-response studies, animals were permitted to respond for each dose of nicotine for 3-5 days; the mean intake over the last 3 sessions for each dose was calculated and used for statistical analysis. Nicotine doses were presented in ascending order with saline last.

Electrophysiological recordings

Adult B6.Cg-Tg(*Chat-COP4*H134R/EYFP*)6Gfng/J mice were sacrificed by cervical dislocation and brains were dissected in chilled (4°C) artificial cerebrospinal fluid (ASCF) containing (in mM): 87 NaCl, 2 KCl, 0.5 CaCl2, 7 MgCl2, 26 NaHCO3, 1.25 NaH2PO4, 25 glucose, 75 sucrose, bubbled with a mixture of 95% O2/5% CO2. 250 µm coronal IPN containing slices were cut with a VT1200S vibratome (Leica, IL, USA), preincubated for 30 min at 37°C and then transferred to the recording solution containing (in mM): 125 NaCl, 2.5 KCl, 2 CaCl2, 1.3 MgCl2, 26 NaHCO3, 1.25 NaH2PO4, 10 glucose, 2 sodium pyruvate, 3 myo-inositol, 0.44 ascorbic acid, bubbled with a mixture of 95% O2/5% CO2. Slices rested in this recording solution at room temperature for at least one hour before they were transferred to the recording chamber. Patch pipettes had resistances of 4–8 MΩ when filled with a solution containing (in mM): 105 K-gluconate, 30 KCl, 10 Hepes, 10 phosphocreatine, 4 ATP-Mg2+, 0.3 GTP (pH adjusted to 7.2 with KOH). Electrophysiological responses were recorded at 33–36 °C with an EPC 10 patch-clamp amplifier and PatchMaster and FitMaster software (HEKA Elektronik, Germany).

Spontaneous miniature EPSCs were recorded from adult WT and *Gpr151*-KO mice at -70 mV in ACSF containing 1 µM TTX, 100 µM Picrotoxin, and 1 µM CGP55845 hydrochloride (all from Tocris, UK).

Light-induced EPSCs were recorded from IPN neurons of *Chat-ChR2* mice and *Chat-ChR2×Gpr151-KO* mice. Two months old adult animals were used in these experiments. Optic fiber was placed above the IPN region of the acute brain slices. Photo stimulation of IPN cell bodies consisted of a single 5ms pulse of 473nm light delivered at a light power of 5mW from the tip of the optic fiber. Picrotoxin (100 µM) or Forskolin (25 µM) were present to block Gabaergic transmission and activate adenylyl cyclase. For assessments of presynaptic release probability, two paired photo stimuli with an interval of 100ms were delivered. Paired pulse responses of IPN neurons were recorded in the presence of Nicotine (1µM) and Picrotoxin (100 µM). The paired pulse ratio was defined as the amplitude of the second EPSC to that of the first EPSC.

Measurement of cAMP levels in dissected IPN brain samples

IPN samples were accurately dissected from WT, *Gpr151-KO* mice and injected mice. An entire IPN per sample was used. Tissues were homogenized with a motorized tissue grinder, lysed with 300µl 0.1 mM HCl for 5 min, and centrifuged (14,000 × g) at 4 °C for 10 min. The concentration of cAMP in the supernatant obtained from mouse extracts was

measured with the Monoclonal Anti-cAMP Antibody Based Direct cAMP ELISA Kit, Non-acetylated Version (NewEast Biosciences Inc) following the manufacturer's instructions.

LANCE cAMP cell-assay measurement

Lance cAMP measurements were done under forskolin stimulation in CHO-K1 parental and GPR151-expressing cell lines. When indicated cells were treated with pertussis toxin (PT) (250 ng/ml) overnight. Cells were grown and assayed in culture reagents (DMEM, FBS, BSA) supplied by Life Technologies,Sigma-Aldrich, and Corning plasticware (Corning). Isobutylmethylxanthine (IMBX) and forskolin were obtained from Tocris Bioscience and Sigma-Aldrich. The LANCE cAMP kit and white opaque 384-well plates were purchased from Perkin Elmer. Cells were detached with Versene (Fisher Scientific) and centrifuged to remove supernatant. Then cells were adjusted to 1000 cell/ µL with HBSS stimulus buffer plus Alexa Flour-647 anti-cAMP antibody. 10 µL of cells were dispersed into 384 well plates with MultiDrop Combi. Forskolin was added with HP D300 digital dispenser. Compound was incubated with cells for 45 mins and detection buffer 10 µL was added. The TR-FRET assay (665nM) was further developed for 1 hour and recorded with Envision Lance dual laser 384 protocols.

SNAP staining on cell lines

GPR151 was labeled with the cell impermeable SNAP dye 549 from New England Biolabs (NEB). SNAP cell staining was done following the manufacturer's instructions. Briefly, dye was dissolved in DMSO at 1mM and further diluted into the cell culture medium to a final concentration of 5µM. For imaging, cells were seeded to Matrigel (Corning) coated glass bottom 384-well plate (Aurora) overnight. Then, the medium was removed and 20µL of 5µM dye was added to each well. The samples were incubated at 37ºC for 20 mins. Afterwards, the dye/medium mixture was discarded and cells were washed twice with fresh cell culture medium and once with PBS (with Ca^{2+} and Mg^{2+}). Finally, cells were imaged either directly or after being fixed with 2% PFD.

Statistical Analysis

Statistical analyses were performed with GraphPad Prism 6.0. Unpaired two-tailed Student t-tests, 2way ANOVA or Repeated Measures (RM) 2way ANOVA were used for analyzing most of the data as indicated in figure legends. See Table S3 for details of statistical analysis. Results are presented as means ± S.E.M.

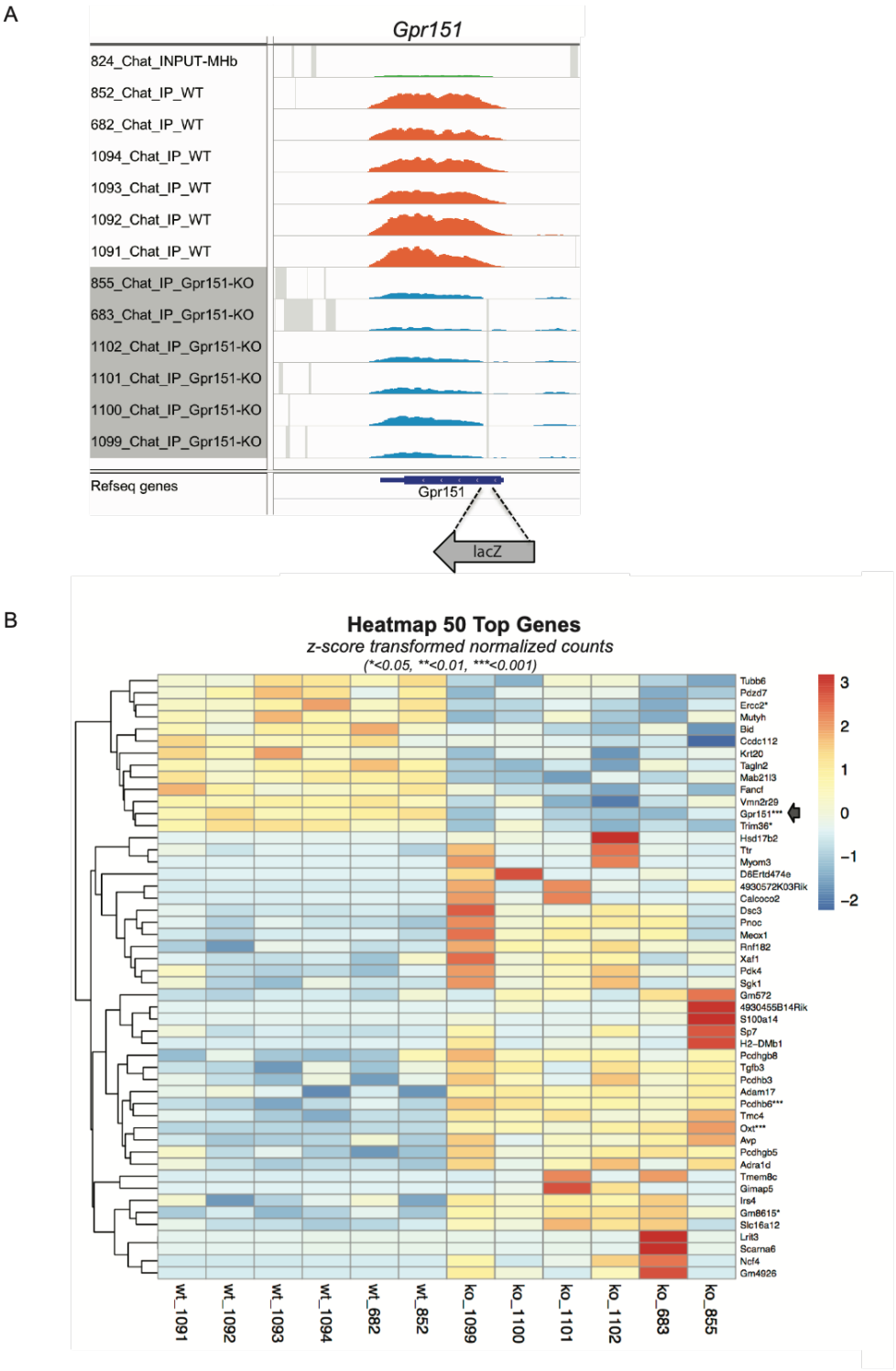

Figure S1: Related to Figure 1

(A) Integrative genome viewer (IGV) of TRAP data collected from the MHb of *Chat*-EGFP-

L10a mice crossed to WT or *Gpr151*-KO showing that *Gpr151* is truncated at the beginning of the gene by the lacZ insertion to generate *Gpr151*-KO.
(B) Heat map of the top 50 genes in WT and KO MHb IP samples. *Gpr151* is indicated with an arrow.

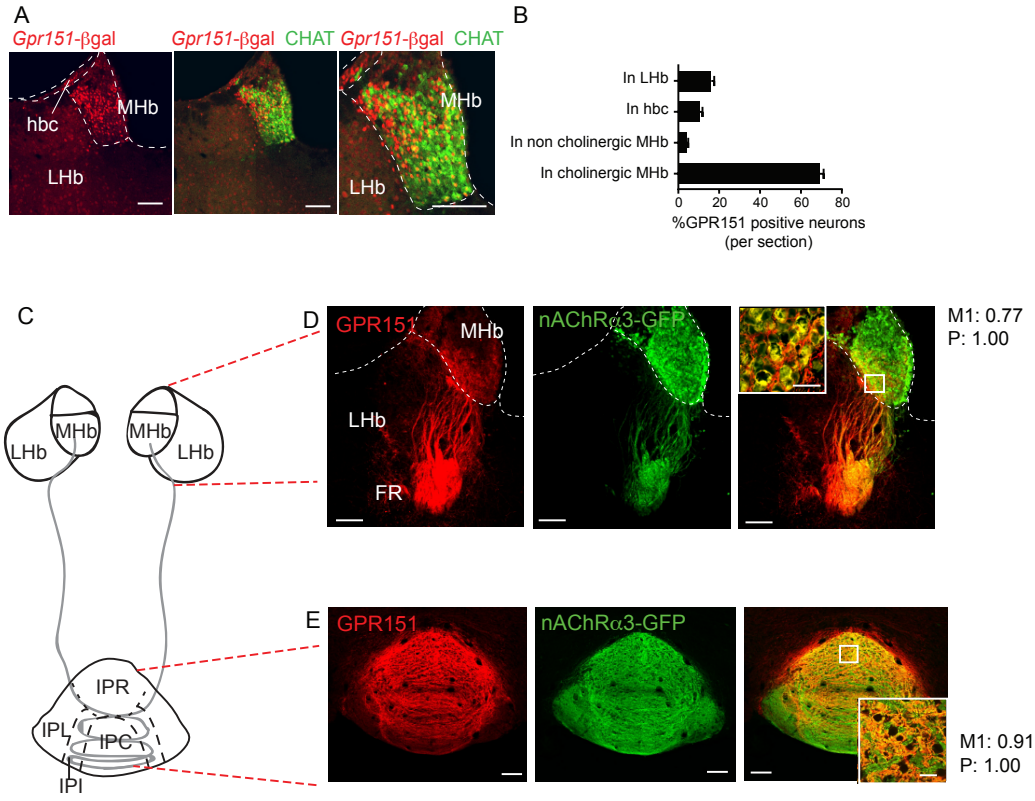

Figure S2: Related to Figure 1

(A) *Gpr151*-KO mice were generated by insertion of the the β-galactosidase (β-Gal) reporter under the *Gpr151* promoter. Coronal section of a *Gpr151*-KO mouse, showing β-Gal and CHAT immunostaining in the habenula. The right panel is a high magnification of the medial habenula (MHb). Scale bar: 100 µm.

(B) Quantification of β-Gal positive neurons in the cholinergic part of MHb (69.06 % ± 2.02); in the non-cholinergic part of MHb (4.30 % ± 0.56), in the habenular commissure (hbc) (10.51 % ± 1.31) and in the lateral habenula (LHb) (16.14 % ± 1.44) (n=39 habenulae from 3 different mice).

(C) Schematic diagram of the habenula-IPN pathway. MHb neurons project along the fasciculus retroflexus to the IPN, where they terminate in a zig-zag pattern.

(D-E) Coronal section of the habenula (D) and IPN (E) showing double immunostaining of GPR151 (red) and nAChRα3-GFP (green) in Tabac mice expressing the Chrnβ4-α3-eGFP-α5 gene cluster. The Manders' colocalization index (M1) and the significance of correlation (P) were measured on the high magnification picture of the indicated square

area. Scale bar: 100 μm for low magnification pictures, 20 μm for high magnification pictures. Colocalization of GPR151 and nAChRα3-GFP was observed in the lateral part of MHb and in the IPR.

Data are represented as mean ± SEM.

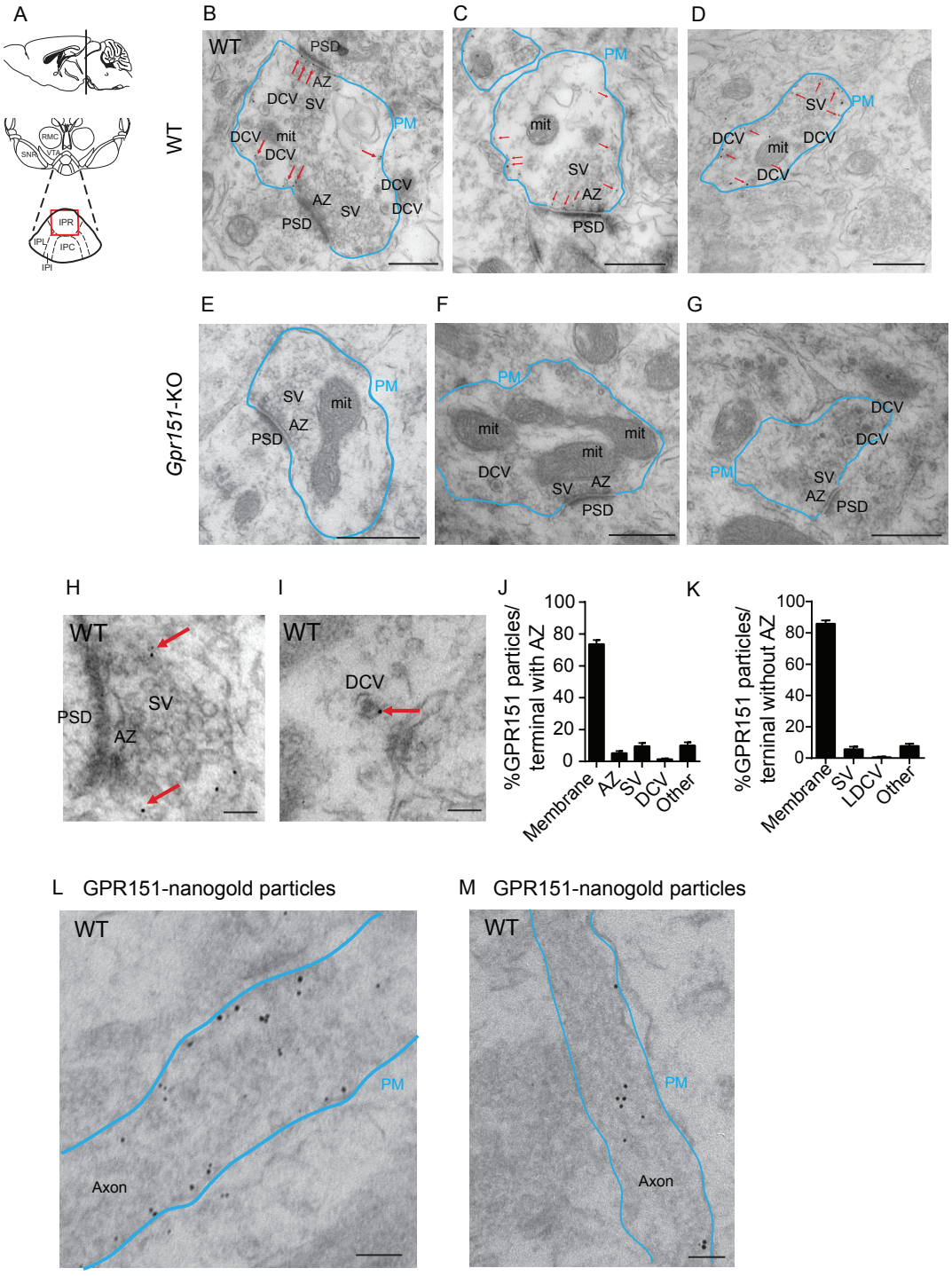

Figure S3. Related to Figure 1

(A) Schematic of the brain area dissected for EM. (IPR: rostral, IPL: lateral, IPI: intermediate, IPC: central subnucleus of the IPN).

(B-D) Representative micrographs of pre-embedding immunogold EM analyses showing GPR151 immunogold particles at habenular terminals of WT mice indicating synaptic vesicles (SV) close to the active zone (B,C) or without the active zone on the plane of the picture (D). The area of the presynaptic terminal is delineated in blue. GPR151 nanogold particles were mainly located at the plasma membrane (PM). Scale bar: 500 nm. (DCV, dense core vesicle, mit, mitochondria).

(E-G) Representative micrographs of pre-embedding immunogold EM analyses showing the absence of GPR151 nanogold particles in presynaptic terminals of *Gpr151*-KO mice. The area of the presynaptic terminal is delineated in blue. Scale bar: 500 nm.

(H-I) Representative micrographs showing GPR151 immunogold particles at the membrane of SVs (H) and DCV (I). Scale bar: 100 nm.

(J) Quantitative analysis of GPR151 pre-embedding immunogold electron micrographs shows that within a synaptic terminal, GPR151 is mostly at the membrane (73.63% ± 2.54) but can also be found at the AZ (5.19 % ± 1.33) and, in association with SV (9.66% ± 1.890); DCV is (1.39% ± 0.51); and other structures (10.11% ± 1.95) (n=50 terminals from 3 WT mice, total of 999 particles).

(K) Quantitative analysis of GPR151 pre-embedding immunogold electron micrographs of synaptic terminals with SV, without the active zone on that plane. The percentage of GPR151 nanogold particles per terminal located on the membrane is 85.87% ± 2.14; in association with SV is 5.7% ± 1.5; in association with DCV is 0.6% ± 0.34; and in other unidentified structures is 7.81 ± 1.31 (n=46 terminals from 3 WT mice, total of 864 particles).

(L-M) Transversal sections of habenular axons showing GPR151 immunogold particles at the membrane and inside the axon along the microtubules being transported towards the terminal. The membrane of the axon is delineated in blue. Scale bar: 100 nm.

Data are represented as mean ± SEM.

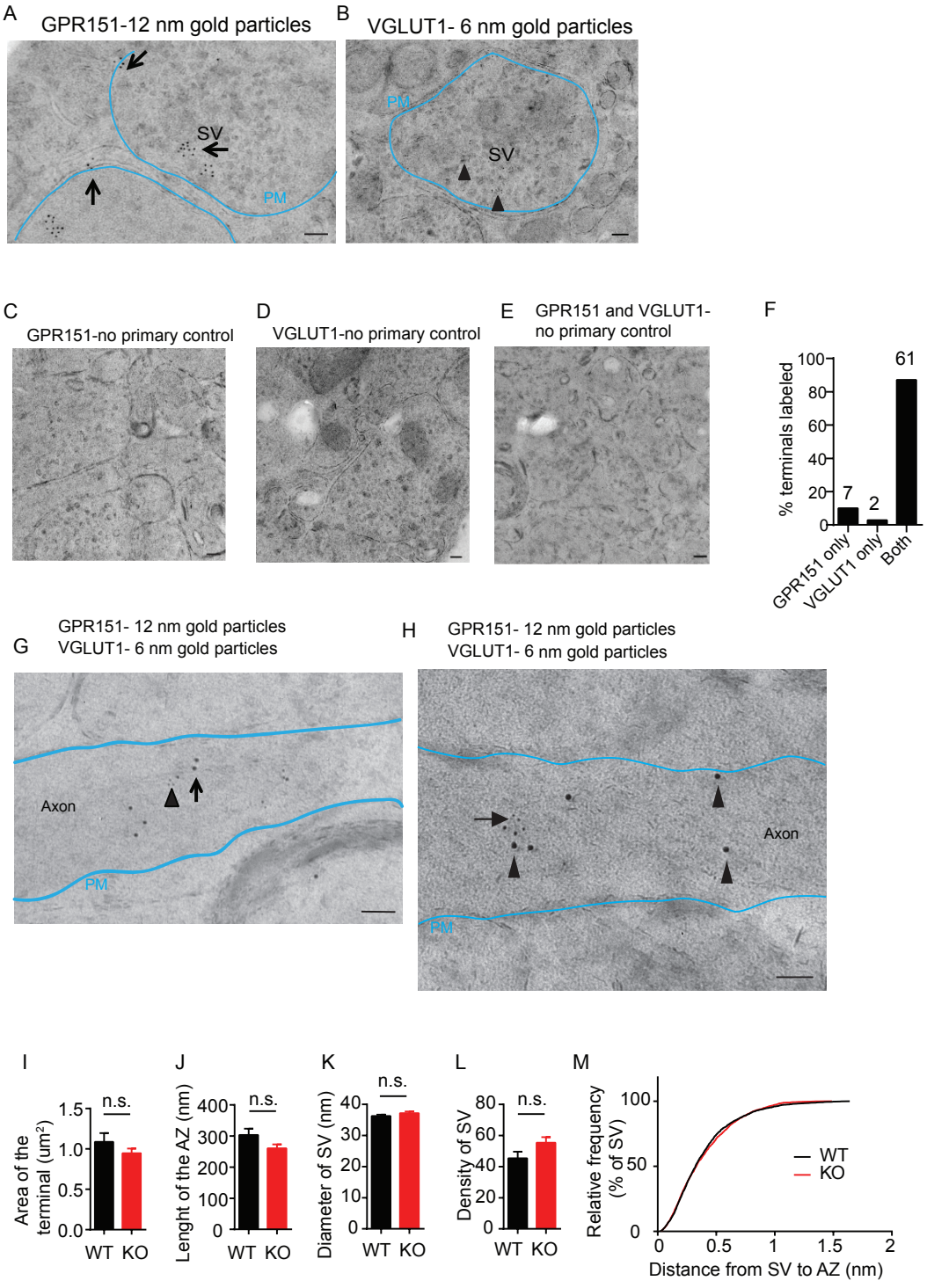

Figure S4. Related to Figure 1.

(A-B) Immunogold particles for GPR151 (12 nm, arrows) and VGLUT1 (6 nm, arrowheads) are localized at presynaptic membranes and SVs in single post- embedding EM

experiments. The area of the presynaptic terminal is delineated in blue. Scale bar: 100 nm.

(C-E) Control experiments of single and double post-embedding labeling of GPR151 and VGLUT1 in the IPR of WT mice. Sections were treated following the same procedure while omitting the primary antibody. Scale bar: 100 nm.

(F) Quantification of the double-postembedding labeled terminals showing the number of terminals labeled only with GPR151, VGLUT1 or both and corresponding percentages. A total of 70 terminals labeled (out of 236) from 3 WT mice were analyzed.

(G-H) Transversal sections of habenular axons showing GPR151 (12 nm) and VGLUT1 (6 nm) particles at higher magnification. The membrane of the axon is delineated in blue. Scale bar: 100 nm.

(I-M) WT and *Gpr151*-KO mice show no significant differences in synaptic terminal area, length of the active zone and synaptic vesicle diameter, density, and distance to the AZ (n=45 terminals from 3 different WT and from 3 different *Gpr151*-KO mice were analyzed.) ($n \geq 45$, unpaired t-test, Table S3).

Data are represented as mean ± SEM.

A

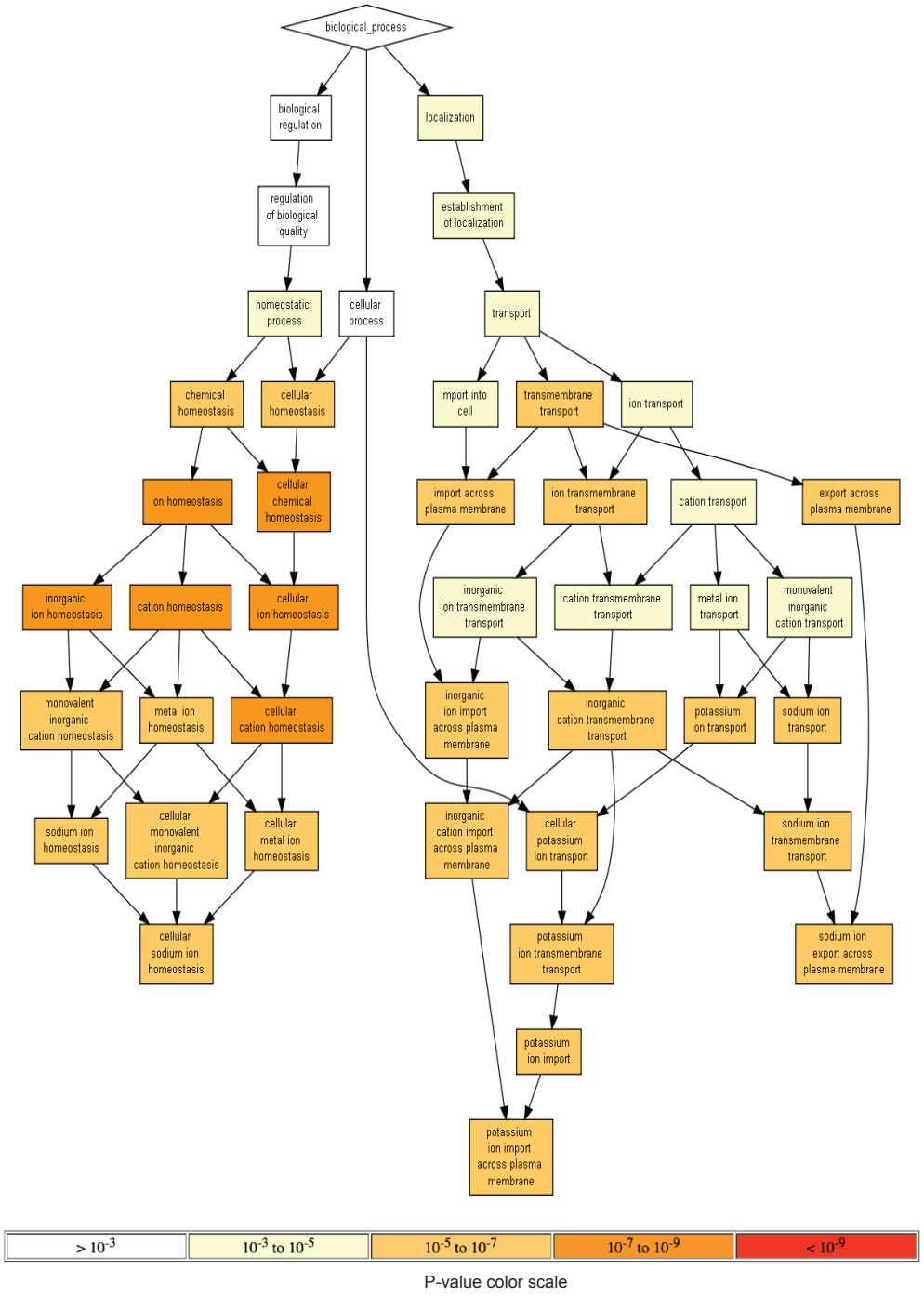

Figure S5. Related to Figure 2

(A) Gene ontology analysis showing the biological processes of the proteins co-immunoprecipitated with GPR151 in WT mice identified by mass spectrometry (See also Table S1).

A

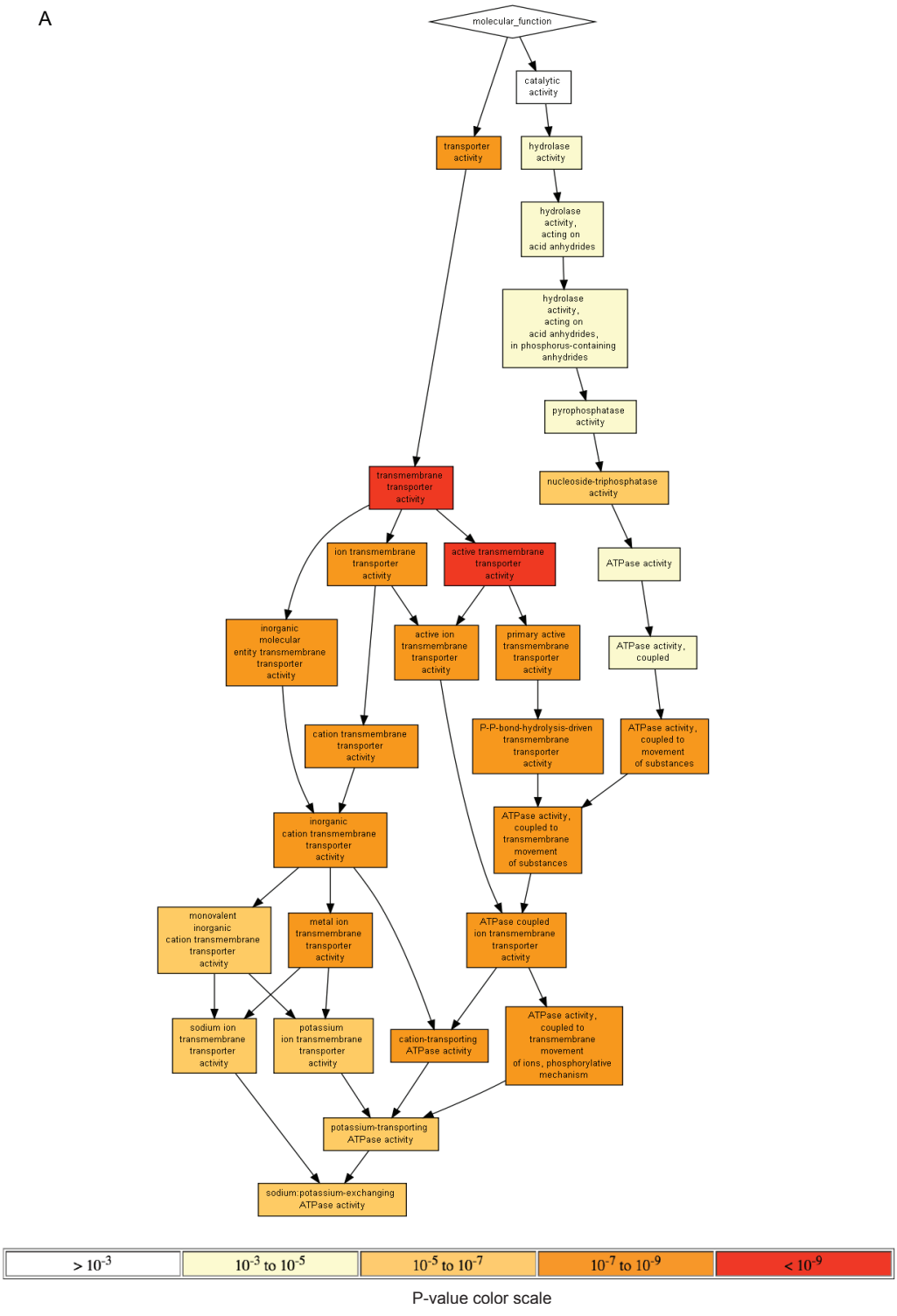

Figure S6. Related to Figure 2

(A) Gene ontology analysis showing the molecular functions of the proteins co-immunoprecipitated with GPR151 in WT mice identified by mass spectrometry (See also Table S1).

A

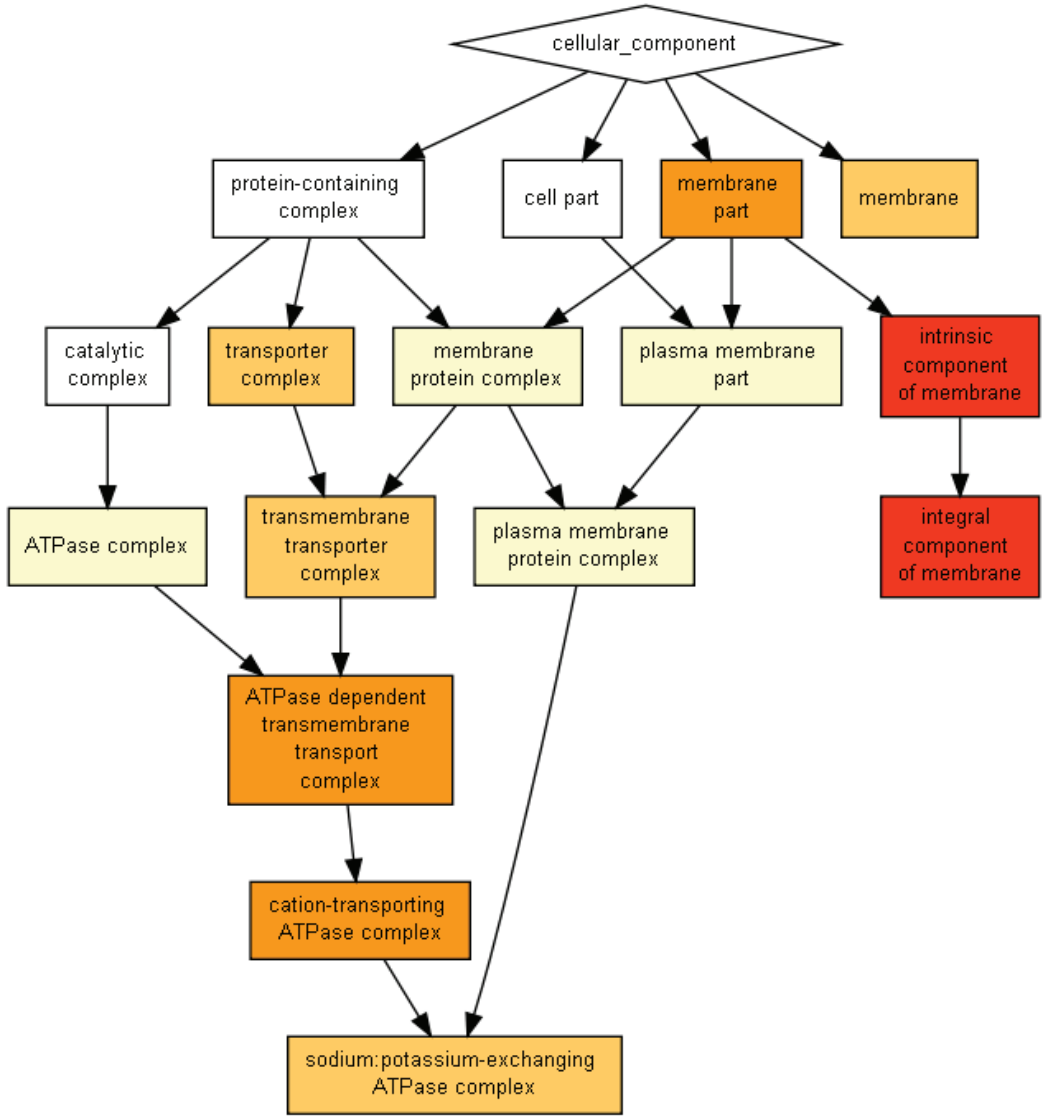

Figure S7. Related to Figure 2

(A) Gene ontology analysis showing the cellular component of the proteins co-immunoprecipitated with GPR151 in WT mice identified by mass spectrometry (See also Table S1).

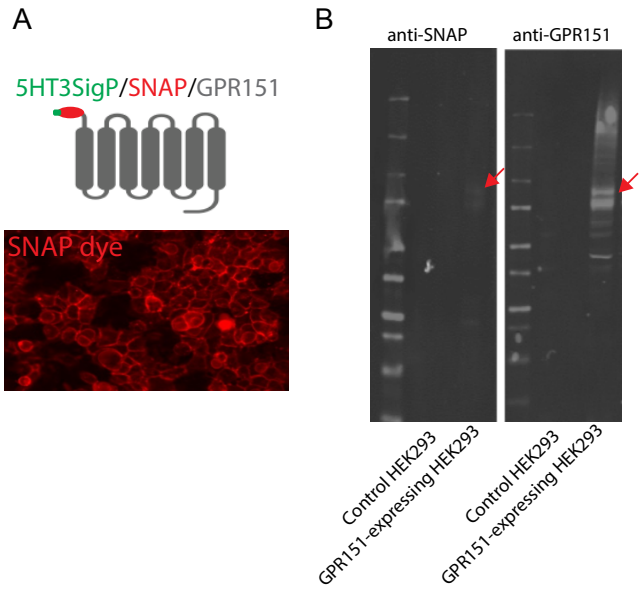

Figure S8. Related to Figure 2

(A) A stable cell line expressing GPR151 with an N-terminus 5HT3 signal peptide to enhance membrane expression [17, 18] and a SNAP-tag to monitor surface expression [19] was generated. Staining with the cell impermeable SNAP dye 549 shows GPR151 expression at the surface in HEK293 stable cell clone.

(B) Whole-length pictures of western blots of control or 5HT3SigP-SNAP-GPR151 transfected HEK293 cells with anti-SNAP (left panel) and anti-GPR151 (right panel) antibodies. The theoretical molecular weight for 5HT3SigP-SNAP-GPR151 is around 66kD, while the western blot results show a molecular weight between 70-100kD because of glycosylation.

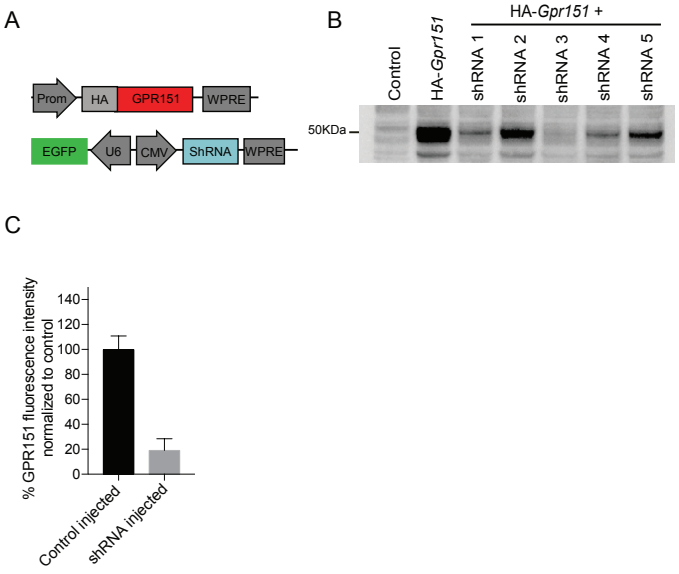

Figure S9. Related to Figure 2

(A) Schematic representation of the lentiviral construct encoding *Gpr151*-HA-tagged and the lentiviral bipromoter construct expressing EGFP and shRNA against *Gpr151*.

(B) Western blot analysis of non-transduced HEK293T cells (line1), transduced with HA-*Gpr151* alone (line 2) or together with 5 different shRNAs against *Gpr151* (lines 3-7). GPR151 was detected in line 2 (47 kDa: GPR151) and was not observed in line 5, indicating that shRNA3 was efficient at knocking-down *Gpr151* in transduced cells.

(C) Quantification of GPR151 fluorescence intensity of IPN sections of 5 WT mice injected in the MHb with LV-scramble (control-injected) and 5 WT mice injected with LV-shRNA against *Gpr151* (shRNA3). The injection of shRNA knocks-down 80% of *Gpr151* expression (control injected: 100 ± 11, n=5 sections from 5 different mice. shRNA injected: 19 ± 9, n=5 sections from 5 different mice).

Data are represented as mean ± SEM.

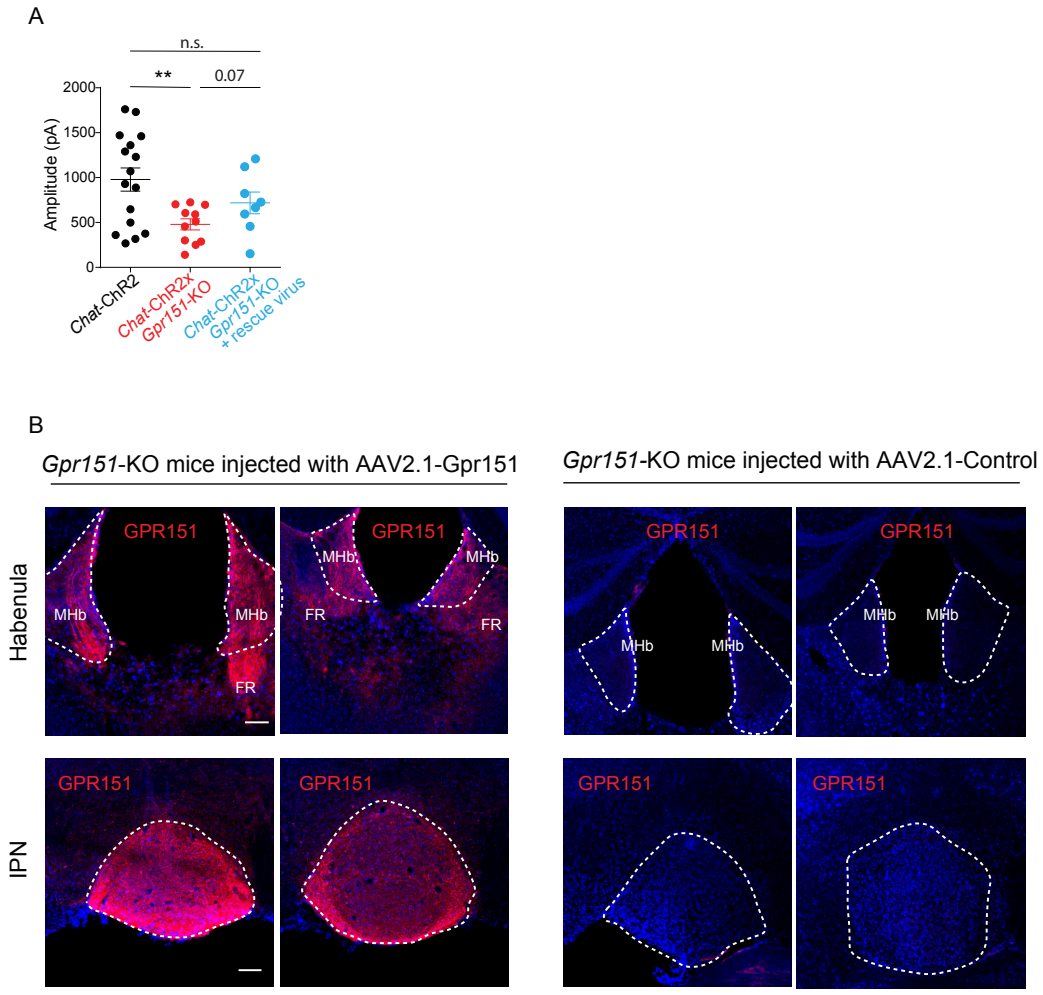

Figure S10. Related to Figure 3

(A) The amplitude of the first blue light evoked EPSC is reduced in Chat-ChR2xGpr151-KO mice (red) compared to Chat-ChR2 mice (black) and partially restored by viral re-expression of GPR151 (blue) (n=16 Chat-ChR2, 11 Chat-ChR2xGpr151-KO, 8 rescue, unpaired t-test, p=0.07 Chat-ChR2xGpr151-KO vs rescue). Data are represented as mean ± SEM. See Table S3 for details of statistical analysis.

(B) GPR151 immunostaining of habenula and IPN coronal sections of 2 different *Gpr151*-KO mice injected in the MHb with AAV2/1-Gpr151 (to rescue expression) and 2 different *Gpr151*-KO mice injected with AAV2/1-control virus. Scale bar: 100um.

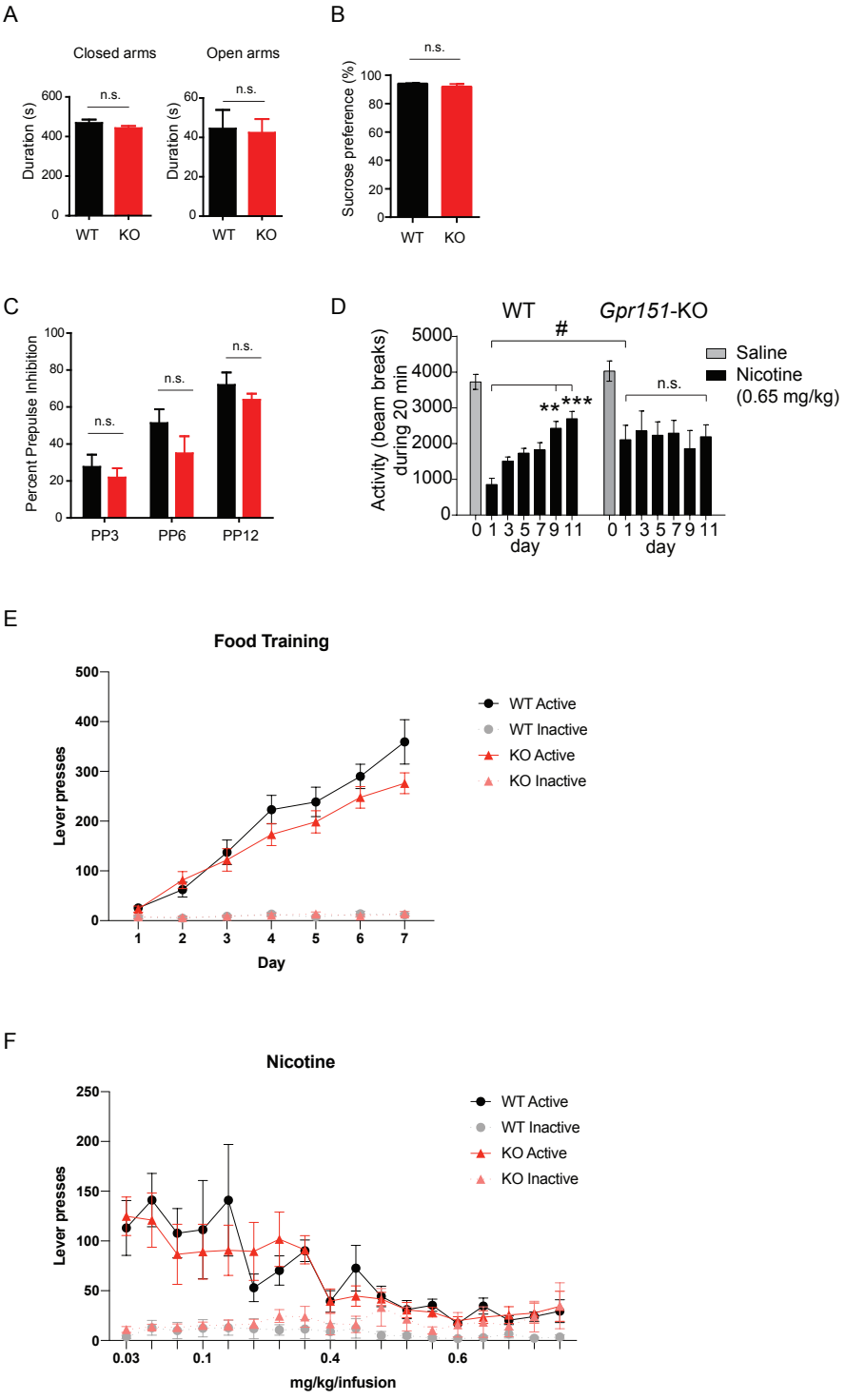

Figure S11. Related to Figure 4

(A) Anxiety-like behavior, measured in the elevated plus maze, was not significantly different in *Gpr151*-KO compared to WT mice. The time spent in the closed and open arms was similar between genotypes (Closed arms: WT=468.8 ± 17.10, n=8; KO=442.3 ±

10.91, n=12, unpaired t-test, p=0.18. Open arms: WT=44.49 ± 9.48, n=8, KO= 42.37 ± 6.94, n=12, unpaired t-test p=0.85).

(B) Anhedonia-like measured with the sucrose preference test was not different between WT and *Gpr151*-KO mice (WT=94.11 ± 0.20, n=10; KO=91.91 ± 1.78, n=10, unpaired t-test, p=0.23).

(C) *Gpr151*-KO mice exhibited normal percent prepulse inhibition of the acoustic startle response across prepulse (PP) intensities (3, 6, 12 dB above background) (n=8-12, 2-way ANOVA).

(D) Consecutive daily injections of nicotine induce tolerance to the hypolocomotor effects of nicotine in WT but not in *Gpr151*-KO mice (n=7 per genotype, RM 2-way ANOVA, Bonferroni multiple comparisons #p<0.05 for genotype; Tukey's multiple comparisons test **p<0.01, ***p<0.001 for time).

(E) Active (solid line) and inactive (dotted line) lever presses during food-training (n=12 WT, 14 KO).

(F) Active (solid line) and inactive (dotted line) lever presses during nicotine self-administration (n= 6 WT, 6 KO; Mixed-effects model, Tukey's multiple comparison test).

Data are represented as mean ± SEM. See Table S3 for details of statistical analysis.

Table S1. In vivo Immunoprecipitation + Mass spectrometry experiments

Protein name	Gene name	Description	Function
AT1A2	Atp1a2	Na^+/K^+ transporting ATPase	P-type **ATP**ases, ion active transport using ATP as energy.
AT1A3	Atp1a3		
AT1B1	Atp1b1		
AT1B2	Atp1b2		
AT2A2	Atp2a2	Ca^+ transporting ATPase	
AT2B3	Atp2b3		
AT5B	Atp5b	H^+ transporting ATPase	
SV2A	SV2a	Synaptic vesicle protein 2	Contributes to vesicle priming and also binds **ATP** suggesting that its priming activity could be modulated by synaptic energy levels.
PGRC1	Pgrmc1	Progesterone receptor membrane component	Functional Part of the Glucagon-like Peptide-1 (GLP-1) Receptor Complex [20].
VDAC2	Vdac2	Voltage-dependent anion channel	Mostly in mitochondria but also at the plasma membrane [21] to transport ATP and Ca^+ and regulate synaptic plasticity [22].
RAB14	Rab14	Small GTP Binding Protein	Member of the RAS family.

Table S2. TRAP expression levels (normalized reads) of heterotrimeric G proteins in MHb neurons of WT and *Gpr151*-KO mice crossed to *Chat*-L10-EGFP mice.

G-protein subunit groups	G-alpha subunits genes	WT	*Gpr151*-KO
G-alpha group s	Gnal	45,717	39,650
	Gnas	**111,241**	**107,691**
G-alpha group q	Gnaq	5,660	6,458
	Gna11	6,920	6,352
	Gna14	3	3
	Gna15	6	2
G-alpha group i	Gnai1	3,829	5,558
	Gnai2	4,471	4,571
	Gnai3	1,574	1,597
	Gnao1	**118,653**	**108,791**
	Gnat1	0	0
	Gnat2	11	16
	Gnat3	0	0
	Gnaz	3,241	3062
G-alpha group 12/13	Gna12	733	688
	Gna13	3,687	3588
G-beta	**Gnb1**	**83,874**	**81,584**
	Gnb2	441	555
	Gnb3	93	78
	Gnb4	1,520	1,315
	Gnb5	5,718	5,556
	Gnb1l	111	113
G-gamma	Gngt1	0	0
	Gngt2	17	13
	Gng2	6377	6596
	Gng3	48,965	45,441
	Gng4	229	310
	Gng5	59	47
	Gng7	790	797
	Gng8	22,789	20,111
	Gng10	2,228	2,090
	Gng11	23	35
	Gng12	361	431
	Gng13	21	35

Table S3. Summary of statistical analysis

Figure	Analysis (*Post-hoc* test indicated in figure)	'n' per group	P value
2F	Unpaired t-test WT vs KO	15	WT: 100.0 ± 7.519 KO: 175.8 ± 19.79 p=0.0016
2F	Unpaired t-test Scramble vs shRNA	8-6	Scramble: 100.0 ± 12.17 shRNA: 136.4 ± 13.67 p=0.0710
2D	One-way ANOVA (to compare EC_{50})	2 (technical triplicates)	F (3, 4) = 317.3, p<0.0001
3A	Unpaired t-test	15	WT: -10.94 ± 0.401 KO: -9.876 ± 0.4273, n=15 p=0.08
3B	Unpaired t-test	14-15	WT: 3.568 ± 0.6513 KO: 6.183 ± 0.7025, n=15 p=0.01
3F	Unpaired t-test	16-11	WT: 978.4 ± 129.1 KO: 478.8 ± 62.01 p=0.0056
3G	Unpaired t-test	6-4	WT Forsk: 1615 ± 155.8 KO Forsk: 390.3 ± 153.6 p=0.0007
3F-G	Unpaired t-test	16-6	WT: 978.4 ± 129.1 WT Forsk: 1615 ± 155.8 p=0.0128
3J	Kruskall Wallis test	17-8-8-10	Kruskall Wallis statistic = 7.625 p = 0.0544
4A	Repeated Measures 2-way ANOVA	7	Interaction F(4, 48) = 3.462, p = 0.0145 Time F(4, 48) = 66.50, p < 0.0001 Genotype F(1, 12) = 6.315, p = 0.0273

4B	Repeated Measures 2-way ANOVA	7-8	Interaction F(12, 96) = 3.672, p = 0.0001 Nicotine concentration F(3, 96) = 175.9, p<0.0001 Genotype F(4, 32) = 4.875, p = 0.0035
4C	Repeated measures 2-way ANOVA	10	Interaction F (1, 18) = 7.579, p = 0.0131 Drug F (1, 18) = 53.89, p < 0.0001 Genotype F (1, 18) = 8.898, p = 0.0080
4D	Repeated measures 2-way ANOVA	4-8	Interaction F (4, 40) =4.431, p = 0.0047 Dose F (4, 40) = 32.13, p < 0.0001 Genotype F (1, 10) = 1.406, p = 0.2632
4E	Repeated measures 2-way ANOVA	4-8	Interaction F (3, 30) = 19.35, p < 0.0001 Dose F (3, 30) = 131.9, p < 0.0001 Genotype F (1, 10) = 16.34, p = 0.0024
4G	Unpaired one-tailed t-test WT vs KO	9-12	WT: 1.32 ± 0.24 KO: 2.48 ± 0.35 p=0.009
4G	Unpaired one-tailed t-test KO Control vs KO Rescue	6	KO Control: 3.62 ± 0.79 KO Rescue: 2.24 ± 0.44 p=0.08
S4I	Unpaired t-test	45	WT: 1.08 ± 0.10 KO: 0.94 ± 0.05 p=0.25
S4J	Unpaired t-test	45-55	WT: 303.5 ± 20.11 KO: 260.6 ± 12.47 p=0.07
S4K	Unpaired t-test	236-144	WT: 36.25 ± 0.47 KO: 37.17 ± 0.54 p=0.21
S4L	Unpaired t-test	45	WT: 45.37 ± 4.29 KO: 55.43 ± 3.51 p=0.07
S4M	Kolmogorov–Smirnov test	1818-2105	p>0.05
S10A	Unpaired t-test	11-8	KO: 478.8 ± 62.01 Rescue: 718.4 ± 12 p=0.07

S11C	2-way ANOVA	8-12	Interaction F (2, 54) = 0.3371, P = 0.7154 Prepulse (PP) F (2, 54) = 20.19, P < 0.0001 Genotype F (1, 54) = 3.257, P = 0.0767
S11D	Repeated Measures 2-way ANOVA	7	Interaction F(6, 72) = 2.828, p = 0.0158 Time F(6, 72) = 14.83, p < 0.0001 Genotype F(1, 12) = 1.565, p = 0.2348
S11E	Mixed-effects model	12, 14	Interaction F (18, 286) = 31.42, p < 0.0001 Time F (2.768, 131.9) = 99.53, p < 0.0001 Genotype F (3, 48) = 52.12, p < 0.0001
S11F	Mixed-effects model	6	Interaction F (51, 334) = 2.946, p < 0.0001 Time F (3.673, 72.16) = 7.645, p < 0.0001 Genotype F (3, 30) = 8.532, p = 0.0003

Dataset S1 (separate file). MaxQuant analysis of the GPR151 co-immunoprecipitations in WT and *Gpr151*-KO mice.

Dataset S2 (separate file). Differential expression analysis of TRAP data collected from the MHb of Chat-EGFP-L10a mice crossed to WT or Gpr151-KO

References

1. Doyle, J.P., et al., *Application of a translational profiling approach for the comparative analysis of CNS cell types.* Cell, 2008. **135**(4): p. 749-62.
2. Frahm, S., et al., *Aversion to nicotine is regulated by the balanced activity of beta4 and alpha5 nicotinic receptor subunits in the medial habenula.* Neuron, 2011. **70**(3): p. 522-35.
3. Heiman, M., et al., *A translational profiling approach for the molecular characterization of CNS cell types.* Cell, 2008. **135**(4): p. 738-48.
4. Gorlich, A., et al., *Reexposure to nicotine during withdrawal increases the pacemaking activity of cholinergic habenular neurons.* Proc Natl Acad Sci U S A, 2013. **110**(42): p. 17077-82.
5. Frahm, S., et al., *An essential role of acetylcholine-glutamate synergy at habenular synapses in nicotine dependence.* Elife, 2015. **4**.
6. Dunn, K.W., M.M. Kamocka, and J.H. McDonald, *A practical guide to evaluating colocalization in biological microscopy.* Am J Physiol Cell Physiol, 2011. **300**(4): p. C723-42.
7. Manders, E.M.M., F.J. Verbeek, and J.A. Aten, *Measurement of co-localization of objects in dual-colour confocal images.* J Microsc, 1993. **169**: p. 375-382.
8. Zinchuk, V. and O. Grossenbacher-Zinchuk, *Quantitative colocalization analysis of fluorescence microscopy images.* Curr Protoc Cell Biol, 2014. **62**: p. Unit 4 19 1-14.
9. Costes, S.V., et al., *Automatic and quantitative measurement of protein-protein colocalization in live cells.* Biophys J, 2004. **86**(6): p. 3993-4003.
10. Rappsilber, J., M. Mann, and Y. Ishihama, *Protocol for micro-purification, enrichment, pre-fractionation and storage of peptides for proteomics using StageTips.* Nat Protoc, 2007. **2**(8): p. 1896-906.
11. Cox, J., et al., *Andromeda: a peptide search engine integrated into the MaxQuant environment.* J Proteome Res, 2011. **10**(4): p. 1794-805.
12. Schwanhausser, B., et al., *Global quantification of mammalian gene expression control.* Nature, 2011. **473**(7347): p. 337-42.
13. Dobin, A., et al., *STAR: ultrafast universal RNA-seq aligner.* Bioinformatics, 2013. **29**(1): p. 15-21.
14. Anders, S., P.T. Pyl, and W. Huber, *HTSeq--a Python framework to work with high-throughput sequencing data.* Bioinformatics, 2015. **31**(2): p. 166-9.
15. Love, M.I., W. Huber, and S. Anders, *Moderated estimation of fold change and dispersion for RNA-seq data with DESeq2.* Genome Biol, 2014. **15**(12): p. 550.
16. Benjamini, Y. and Y. Hochberg, *Controlling the False Discovery Rate: A Practical and Powerful Approach to Multiple Testing.* Journal of the Royal Statistical Society. Series B, 1995. **57**: p. 289-300.

17. Wellerdieck, C., et al., *Functional expression of odorant receptors of the zebrafish Danio rerio and of the nematode C. elegans in HEK293 cells.* Chem Senses, 1997. **22**(4): p. 467-76.
18. Wetzel, C.H., et al., *Specificity and sensitivity of a human olfactory receptor functionally expressed in human embryonic kidney 293 cells and Xenopus Laevis oocytes.* J Neurosci, 1999. **19**(17): p. 7426-33.
19. Ward, R.J., J.D. Pediani, and G. Milligan, *Ligand-induced internalization of the orexin OX(1) and cannabinoid CB(1) receptors assessed via N-terminal SNAP and CLIP-tagging.* Br J Pharmacol, 2011. **162**(6): p. 1439-52.
20. Zhang, M., et al., *Progesterone receptor membrane component 1 is a functional part of the glucagon-like peptide-1 (GLP-1) receptor complex in pancreatic beta cells.* Mol Cell Proteomics, 2014. **13**(11): p. 3049-62.
21. De Pinto, V., et al., *Voltage-dependent anion-selective channel (VDAC) in the plasma membrane.* FEBS Lett, 2010. **584**(9): p. 1793-9.
22. Weeber, E.J., et al., *The role of mitochondrial porins and the permeability transition pore in learning and synaptic plasticity.* J Biol Chem, 2002. **277**(21): p. 18891-7.